Electronic Supplementary Material (ESI) for Soft Matter.

Cavanna, Alvarado. Quantification of the mesh structure of bundled actin filaments

Electronic Supporting Information

Supplementary Figures to the Main Text

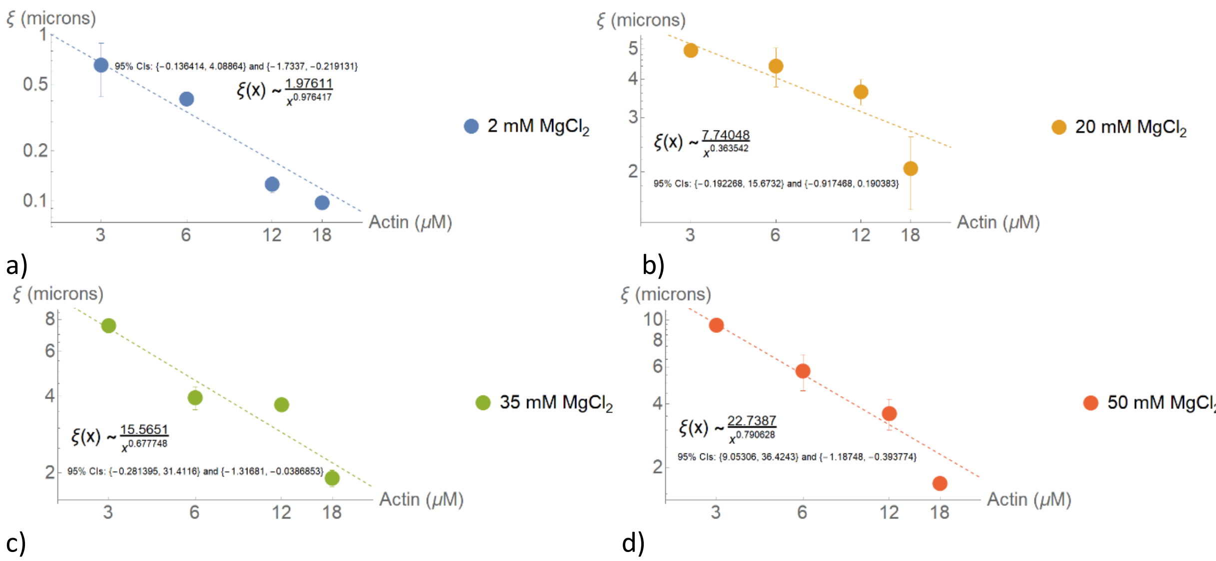

Fig 1: Best-fit lines made by least-square fitting of mesh size against actin concentration for MgCl2-bundled actin networks for each concentration studied (figures a-d). In each figure, the confidence interval is reported for both calculated parameters in the inverse power-law fit.

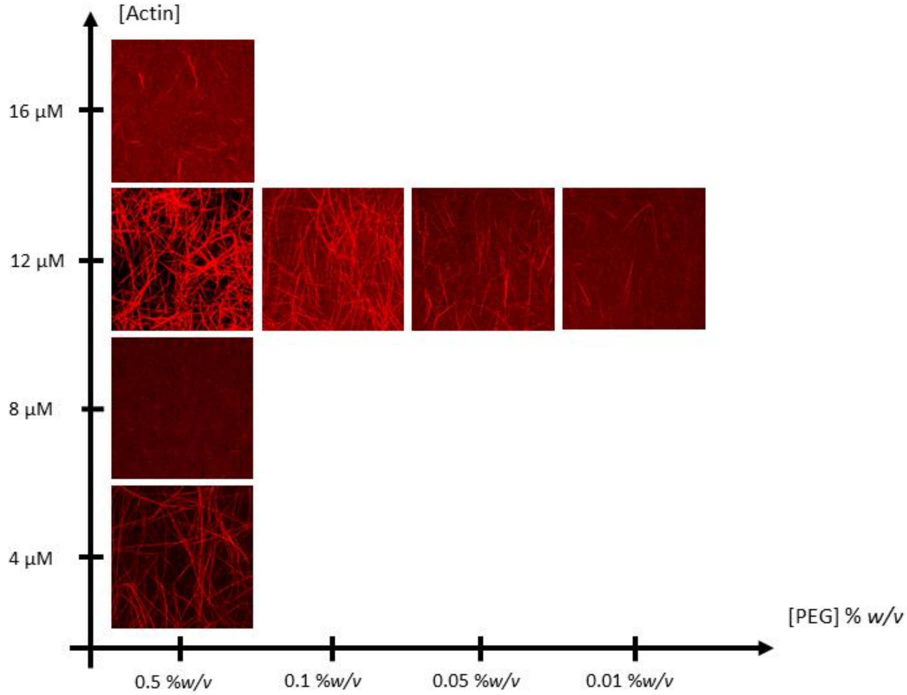

Fig 2: Phase plot of actin and PEG concentrations, down to 0.01% w/v of PEG. Images are projections of a z-stack through 15 µm. The critical concentration begins at 0.5 % w/v of PEG, but bundles exist even below an order of magnitude.

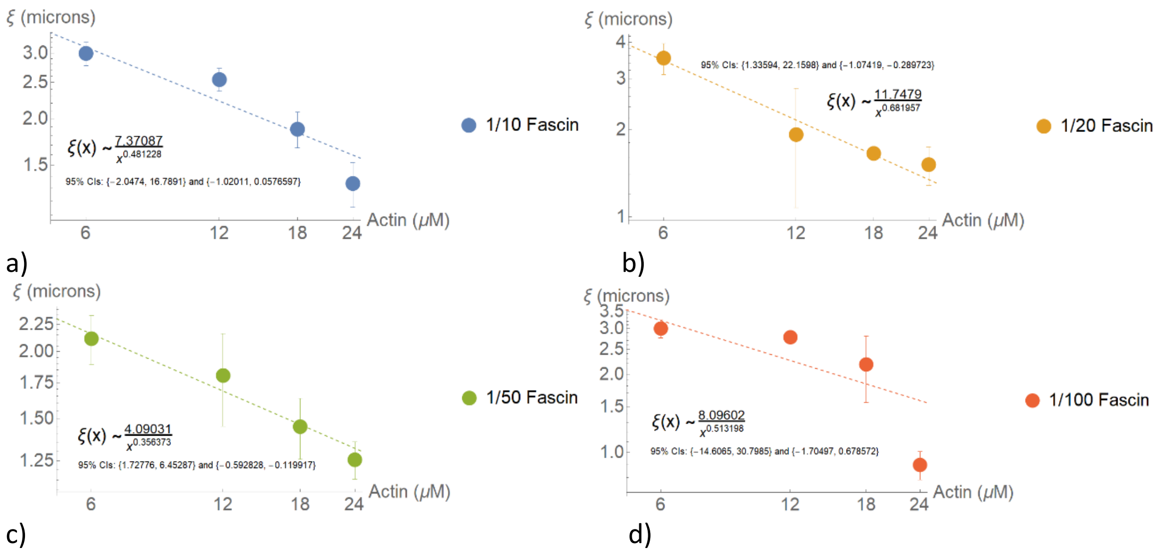

Fig 3: Best-fit lines made by least-square fitting of mesh size against actin concentration for fascin-bundled actin networks for each concentration studied (figures a-d). In each figure, the confidence interval is reported for both calculated parameters in the inverse power-law fit.

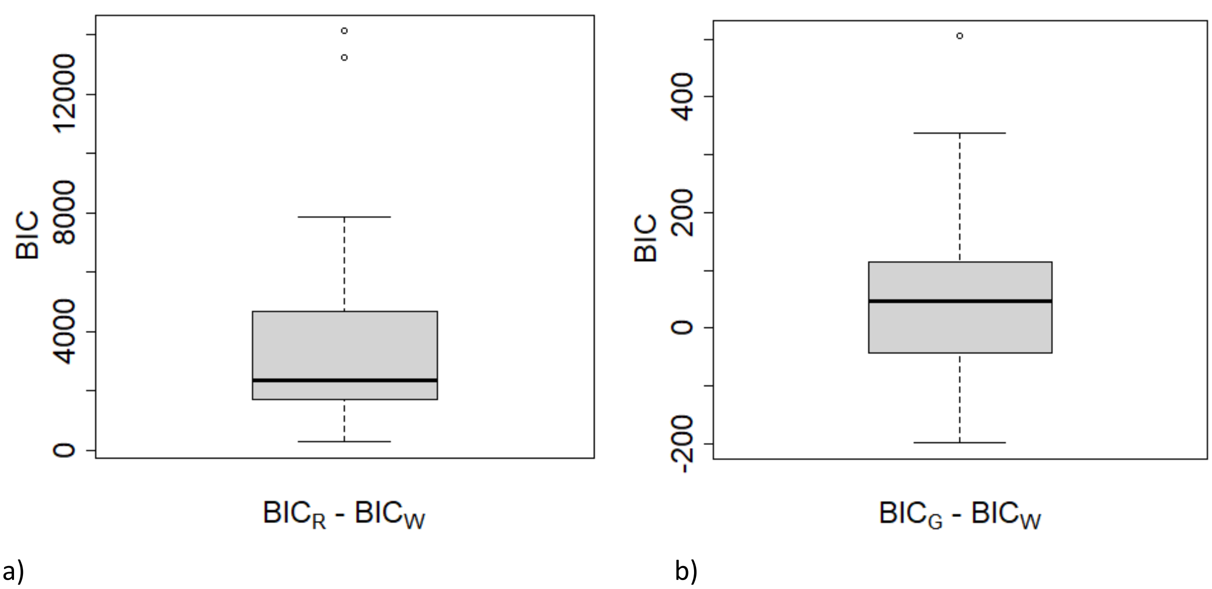

Fig. 4: Weibull distributions are favored over Rayleigh and Gamma distributions for PEG networks. A comparison of a) the calculated BIC difference between the Weibull Distribution and the Rayleigh distribution and b) the calculated BIC difference between the Weibull Distribution and Gamma distribution for PEG-bundled actin networks. Negative BIC values indicate the Weibull distribution is unfavorable compared to Rayleigh/Gamma distributions. Also note the order of magnitude of difference between panel a) and panel b), indicating the Rayleigh distribution is strongly disfavored in comparison to the Weibull. As for the Gamma distribution, it is overall disfavored in comparison to the Weibull, although some samples are preferred over the Weibull, as indicated by some data points with negative values in panel b.

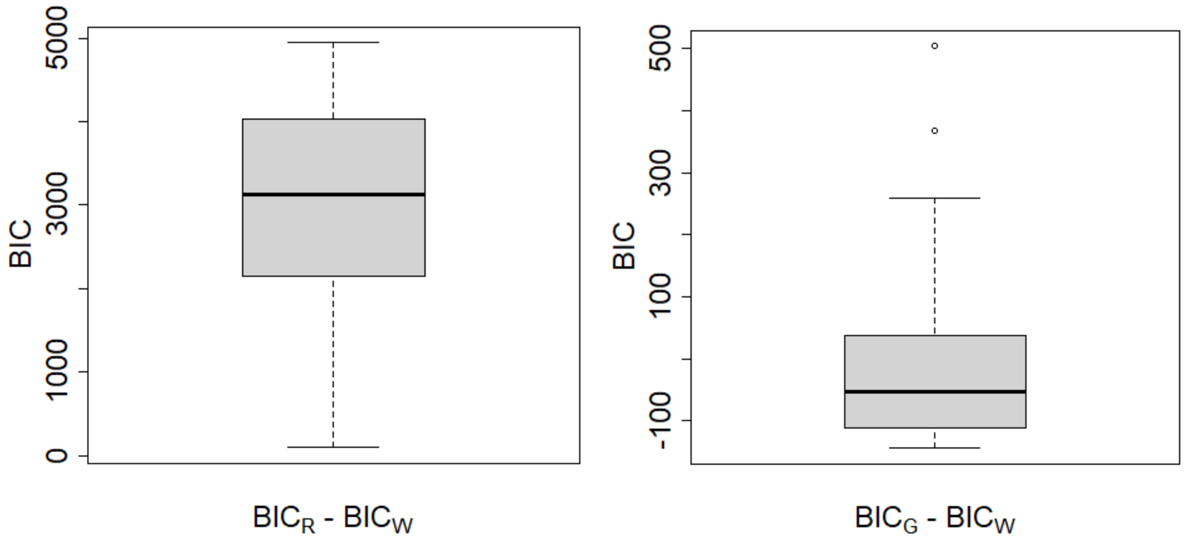

a) b)

Fig. 5: Gamma distributions are favored over Rayleigh and Weibull distributions for MgCl2 networks. A comparison of a) the calculated BIC difference between the Weibull Distribution and the Rayleigh distribution and b) the calculated BIC difference between the Weibull Distribution and Gamma distribution for MgCl2-bundled actin networks. Note that negative BIC values indicate the Weibull distribution is unfavorable compared to Rayleigh/Gamma distributions. Note the order of magnitude of difference between panel a) and panel b), indicating the Rayleigh distribution is strongly disfavored in comparison to the Weibull, while the Gamma distribution is favored in some acquisitions over the Weibull.

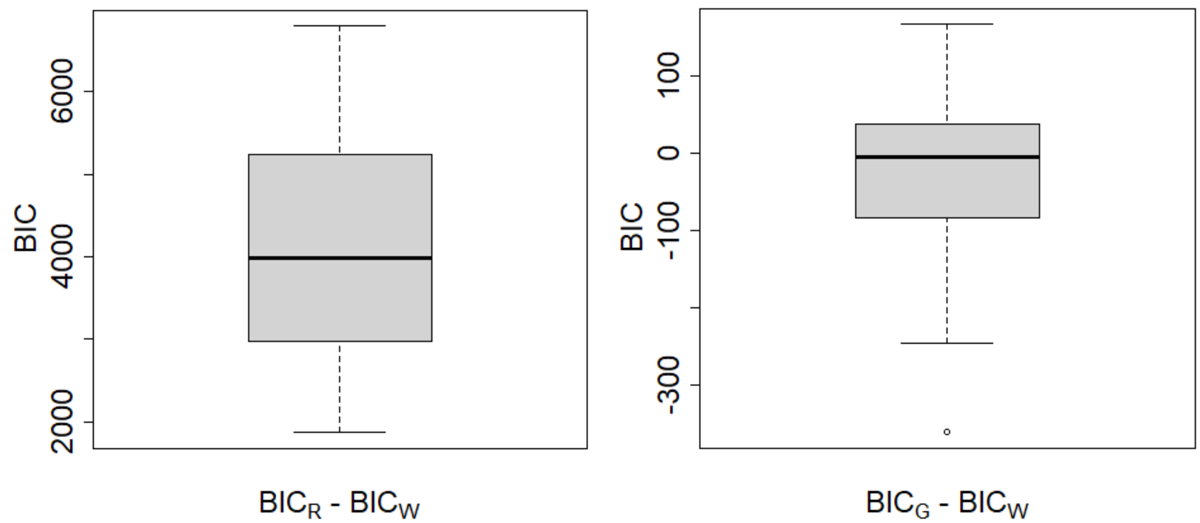

a) b)

Fig. 6: Weibull and Gamma distributions are favored over Rayleigh distributions for alpha-actinin networks. A comparison of a) the calculated BIC differences between the Weibull Distribution and the Rayleigh distribution and b) the calculated BIC difference between the Weibull Distribution and Gamma distribution for alpha-actinin-bundled actin networks. Note that negative BIC values indicate the Weibull distribution is unfavorable compared to Rayleigh/Gamma distributions, and also note the order of magnitude of difference between panel a) and panel b), indicating the Rayleigh distribution is strongly disfavored in comparison to the Weibull, while the Gamma distribution has some images that are preferred over the Weibull.

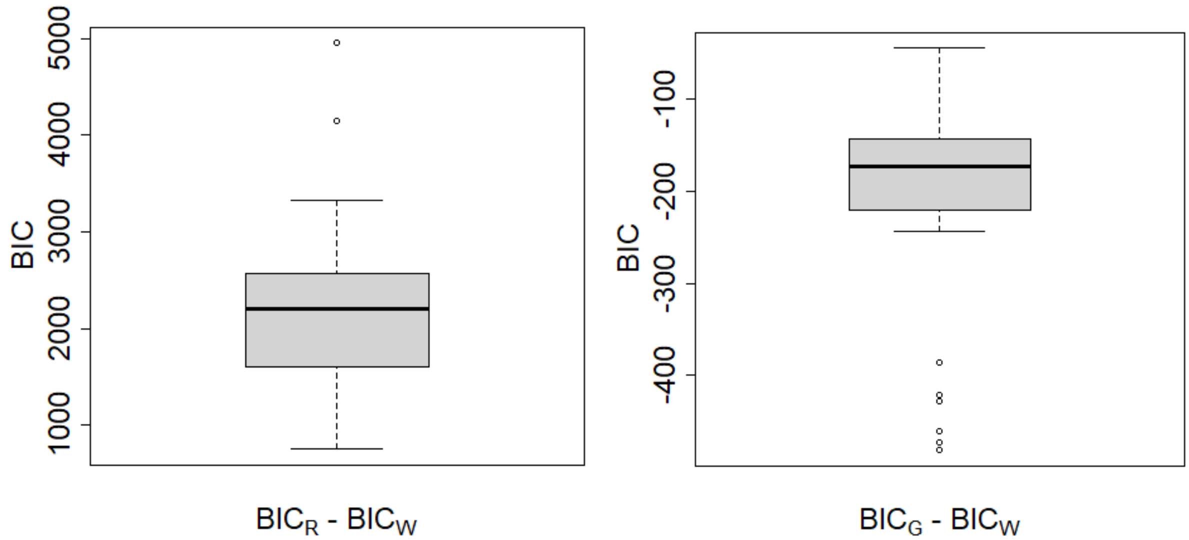

a) b)

Fig. 7: Gamma distributions are favored over Rayleigh and Weibull distributions for fascin networks A comparison of a) the calculated BIC differences between the Weibull Distribution and the Rayleigh distribution and b) the calculated BIC difference between the Weibull Distribution and Gamma distribution for Fascin-bundled actin networks. Negative BIC values indicate the Weibull distribution is unfavorable compared to Rayleigh/Gamma distributions Note panel b returns only negative values for the difference between the Weibull's BIC and the Gamma's BIC – this means the Gamma distribution is exclusively preferred over the Weibull distribution.

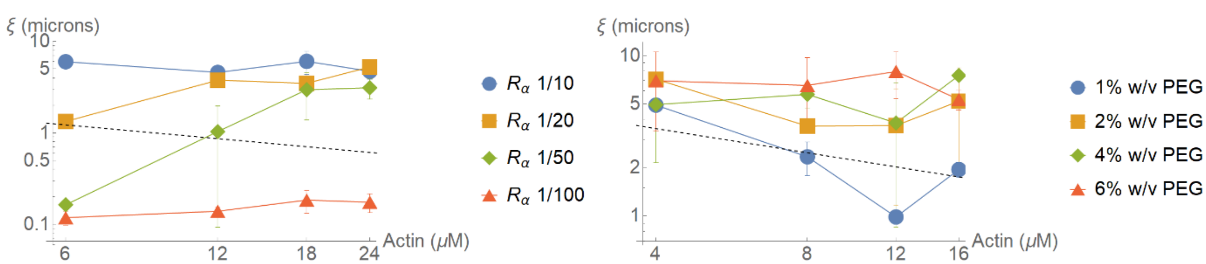

a) b)

Fig 8: Logarithmic plots for mesh size vs. actin concentration for a) α-actinin and b) PEG. Each plot has a dashed line that follows the predicted power law behavior: $\xi \sim x^{-1/2}$. The data do not follow the predicted inverse power law.

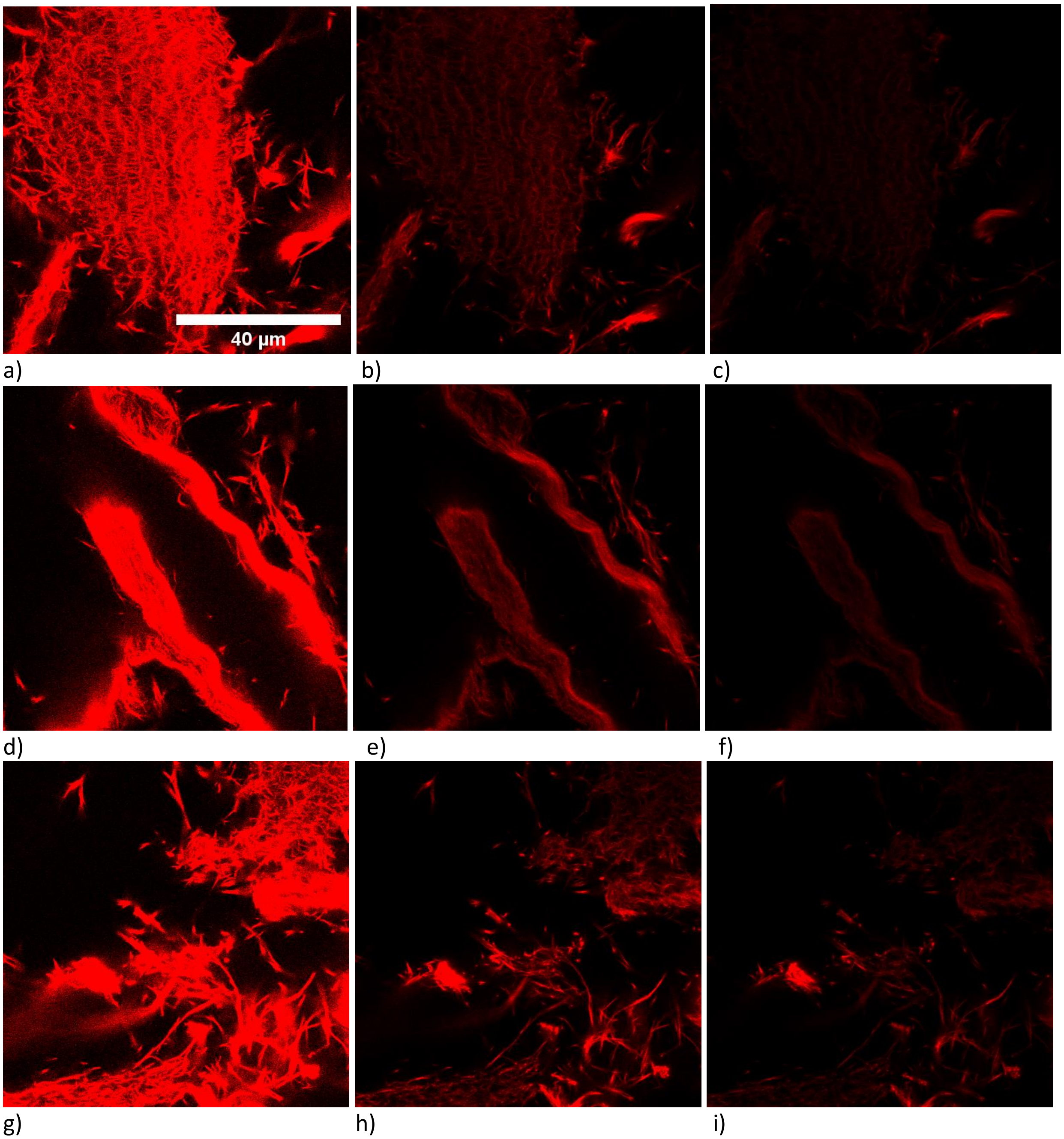

Fig 9: A set of three different aggregates for an [actin] = 12 µM sample, [PEG] = 6%. Note that each aggregate at lower intensities reveals bundles of actin filaments within its structure. These images show that aggregates are composed of bundles which have been driven together via inter-bundle attractive interactions.

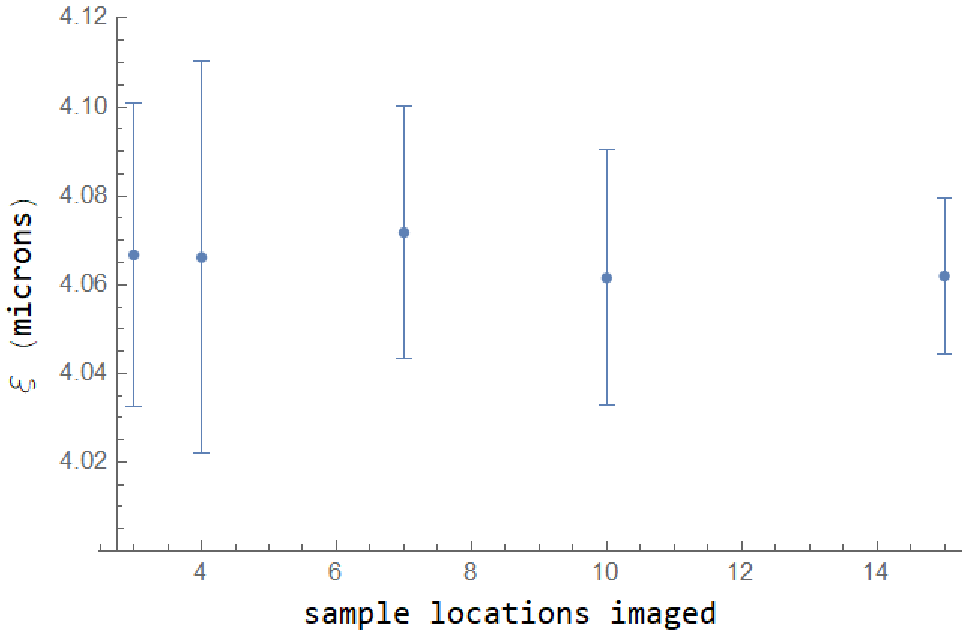

Fig 10: A comparison between mesh sizes generated from 3, 4, 7, 10, and 15 locations in a single sample of actin and alpha-actinin ([actin] = 12μM, R_α = 1/100). The total depth of each slide was 50 μm.

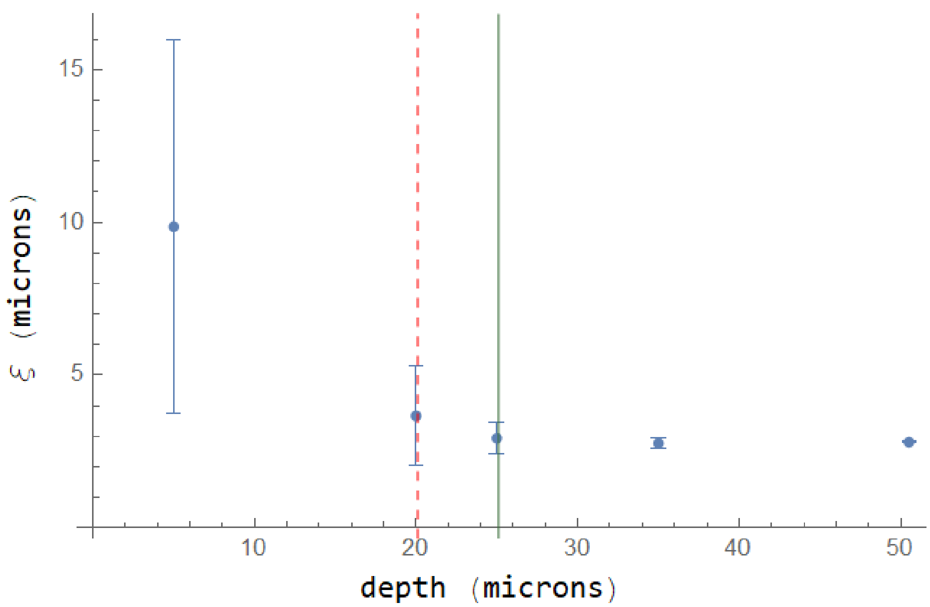

Fig. 11: A comparison between mesh sizes generated from different depths of a *z*-stack, imaged from a single sample of actin and alpha-actinin ([actin] = 12 μM, R_α = 1/100). Depth in microns is represented on the x-axis and mesh size is represented on the y-axis.

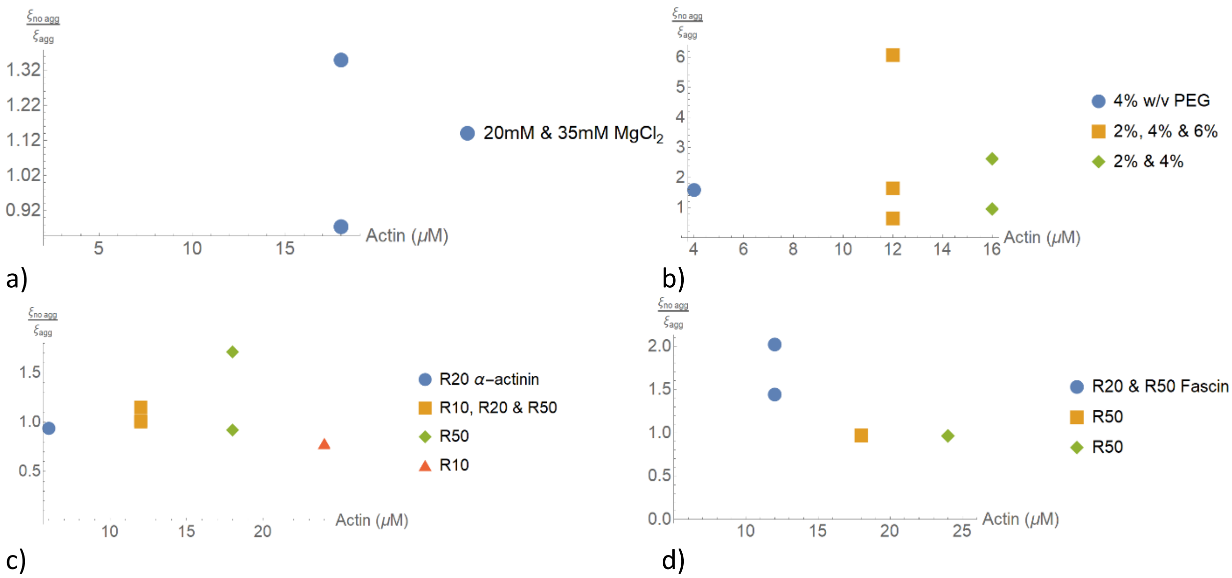

Fig 12: Mesh-size ratios for actin bundles from *z*-stacks with aggregated actin and without aggregated actin for a) MgCl2-bundled actin, b) PEG-bundled actin, c) α-actinin, and d) fascin. We find that the mesh-size ratio is in many cases approximately equal to one, which suggests that the mesh size is not significantly affected by the presence of aggregates. This result is expected given our image analysis routine, which is not sensitive to the presence of aggregates.